Journal of Applied Physics ARTICLE scitation.org/journal/jap

A comparable study of defect diffusion and recombination in Si and GaN

Cite as: J. Appl. Phys. **132**, 045701 (2022); doi: 10.1063/5.0094691
Submitted: 5 April 2022 · Accepted: 25 June 2022 ·
Published Online: 25 July 2022

Xiang-Ru Han,[1] Yang Li,[1] Pei Li,[1] Xiao-Lan Yan,[1] Xiao-Qiang Wu,[2] and Bing Huang[1,3,a)]

AFFILIATIONS

[1]Beijing Computational Science Research Center, Beijing 100193, China
[2]School of Mechanical Engineering, Chengdu University, Chengdu 610106, China
[3]Department of Physics, Beijing Normal University, Beijing 100875, China

[a)]**Author to whom correspondence should be addressed:** bing.huang@csrc.ac.cn

ABSTRACT

Both the static and kinetic properties of defects play fundamental roles in determining the physical properties of semiconductors. Compared to the static properties of defects, a comprehensive understanding of the different defects diffusing in different types of semiconductors is still lacking. In this article, based on extensive first-principles calculations, we have done a comparative study on the diffusion mechanisms of point defects in Si (a typical elemental semiconductor) and GaN (a typical compound semiconductor). The significantly different diffusion mechanisms of vacancies and interstitials in Si and GaN result in significantly different recombination mechanisms, i.e., a novel synergistic effect to accelerate the annihilation of defects is observed in Si but not in GaN, indicating that an efficient self-recovery mechanism can exist in Si but not in GaN. Our results not only explain some experimental observations in Si and GaN under nonequilibrium irradiation conditions but also provide a good example to understand the different kinetic properties of defects in elemental and compound semiconductors.

I. INTRODUCTION

Elemental and compound semiconductors have broad applications in our daily life. As a typical example of elemental semiconductors, silicon (Si) is the foundation for solar cells[1–3] and field-effect transistors[4] in the industry. On the other hand, as a typical example of compound semiconductors, gallium nitride (GaN) has been widely used in solid-state light-emitting devices,[5,6] high electron mobility transistors,[7] power rectifiers, and radiation detectors.[8] In these practical applications, both Si and GaN are unavoidably exposed to different degrees of irradiations, which will introduce various nonequilibrium defects.[9,10] In addition, during the growth and processing of semiconductors, various defects can also be introduced. The electronic states of defects, defect concentrations, and types of defects seriously affect optoelectronic performance and cause the degradation of semiconductor devices.[11–13]

Experimentally, electron paramagnetic resonance, deep-level transient energy spectrum, and positron annihilation spectroscopy have widely been used to characterize the defect species in semiconductors.[14] Theoretically, first-principles density functional theory (DFT) calculations can be used to obtain the related electronic states of defects independent of the experimental data, such as thermodynamic charge state transition levels (CTLs), optical transition levels of defects, and defect formation energy.[15,16] The thermodynamic properties of defects can be analyzed quantitatively by combining theoretical calculations with experiments. The properties of the intrinsic point defects in Si[17,18] and GaN[19,20] have also been studied.

Most of the diffusion processes in semiconductors are assisted by defects, e.g., high-quality growth of host and effective doping at high temperatures and irradiated conditions.[21,22] Besides static defect properties, the kinetic properties of defects can also determine the performance of semiconductor devices. Therefore, it is highly important to understand the dynamic diffusion process of defects in semiconductors.[23–25] Although the intrinsic defects diffusions were mentioned in the previous studies on Si[26–28] and GaN,[29,30] a comprehensive understanding of the dynamic evolution of defects is still lacking, especially for the similarities and differences between Si and GaN. For example, recovery of defects

introduced by electron irradiation is observed in Si, which may be attributed to the recombination of Frenkel defects in Si.[31] In addition, the annihilation of Frenkel defects was also observed in GaN,[32,33] and the disordering rate of the Ga sublattice is smaller than the N sublattice in the low-irradiation damage experiment;[34] however, the mechanism that accounts for the dynamic recombination process of defects in GaN remains largely unclear. Especially, besides Si, GaN is widely considered another important semiconductor system used in irradiation conditions. Therefore, the understanding of the dynamic diffusion process of defects is important for further optimizing the electronic properties of Si and GaN under thermodynamic nonequilibrium conditions.

In this article, based on the first-principles calculations, we have performed a systematic study on the diffusion mechanisms of all the basic point defects in Si and GaN, since point defects with larger formation energies may also form under nonequilibrium irradiation. For vacancy defects, the diffusion barrier of Si vacancy (V_{Si}) is very small, one order of magnitude smaller than that of Ga (V_{Ga}) or N (V_N) vacancies. It indicates that vacancies are much faster diffusors in Si than in GaN. For interstitial defects, Si interstitial (Si_i) diffuses via both direct diffusion and kick-out diffusion mechanisms, and Ga interstitial (Ga_i) diffuses mainly through the direct diffusion mechanism, while N interstitial (N_i) only diffuses via the kick-out diffusion mechanism. Surprisingly, the diffusion barrier of N_i is much larger than that of Ga_i, invaliding the common expectation that smaller atoms are easier to diffuse. This is because N_i can form an unusual dimer with the host N in GaN, which is very difficult to be broken during the diffusion process. The significantly different diffusion mechanisms of vacancies and interstitials in Si and GaN result in significantly different recombination mechanisms. For example, a novel synergistic effect to accelerate the annihilation of defects is observed in Si but absent in GaN, indicating that an efficient self-recovery mechanism can exist in Si but not in GaN, explaining the experimental observations.

II. METHOD

The physical properties of intrinsic defects were studied by performing the first-principles-based density functional theory (DFT) calculations, as implemented in the Vienna *ab initio* Simulation Package (VASP).[35] The projector augmented wave (PAW) method[36] was employed to treat the core electrons, and the Perdew–Burke–Ernzerhof (PBE) functional[37] was chosen to approximate the exchange–correlation functional. The energy cutoff for the plane wave basis was set to be 300 and 520 eV for the calculations of Si and GaN, respectively. To avoid the interactions between the defects and their periodic images, for Si, the conventional cell which contains eight atoms was chosen to be the unit cell, and the $3 \times 3 \times 3$ cubic supercell containing 216 atoms combined with the single Γ point was used to calculate all the properties. For GaN, the primitive cell which contains four atoms was adopted, and the $3 \times 3 \times 2$ wurtzite supercell containing 72 atoms combined with the $3 \times 3 \times 3$ Γ-centered *k*-point mesh was employed to perform the single point defects diffusion. In addition, for other properties of defects in GaN, the cubic cell that contains eight atoms was chosen to be the unit cell to complete the calculations. That is, the diffusion barrier of defect pairs was performed by the single Γ point calculations on a larger $5 \times 3 \times 3$ cubic supercell containing 360 atoms, as well as the defect formation energy and CTLs were performed by the single Γ point calculations on a $3 \times 2 \times 2$ cubic supercell containing 96 atoms using the hybrid functional.[38] All the migration barriers of defects and the evolution of defect pairs were studied using the climbing image nudged elastic band method (CI-NEB),[39] where the image structures were fully relaxed until the force on each atom was $<0.03\,\text{eV Å}^{-1}$. In all calculations, the energy convergence criterion is 10^{-5} eV. We have performed convergence tests on the supercells used for the calculations.

The calculations of the defect formation energy were based on its definition,[15,16]

$$\Delta H_f(\alpha, q) = \Delta E(\alpha, q) + \sum_i n_i \mu_i + qE_F + \Delta E_{align}(\alpha, q), \quad (1)$$

where $\Delta E(\alpha, q) = E(\alpha, q) - E(\text{host}) + \sum_i n_i E_i + qE_{VBM}$. $E(\alpha, q)$ and $E(\text{host})$ represent the total energy of the supercell containing defect and the perfect supercell, respectively. α marks defect, q indicates charge state, n_i is the number of elements, μ_i is the chemical potential of constituent i with energy E_i (i = Si, Ga, N) and E_F is the Fermi level referring to the valence band maximum (E_{VBM}) of the host. $\Delta E_{align}(\alpha, q)$ is the core level difference between the supercell with the defect and the perfect supercell. Based on the formation energy of the point defect, the CTLs of the defect is calculated as

$$\varepsilon(q/q') = \frac{[\Delta E(\alpha, q) + \Delta E_{align}(\alpha, q)] - [\Delta E(\alpha, q') + \Delta E_{align}(\alpha, q')]}{q' - q} - E_{VBM}, \quad (2)$$

which corresponds to the position of the Fermi level where the defect in charge state q and q' have the same formation energy.

III. RESULTS AND DISCUSSION

A. Diffusion mechanisms of individual vacancies in Si and GaN

Vacancy is the most common defect, which has D_{2d} symmetry for V_{Si} in Si and C_{3v} symmetry for V_{Ga}/V_N in GaN. Figure 1(a) shows the calculated energy barriers for V_{Si}, V_{Ga}, and V_N diffusion. In the elemental semiconductor Si, V_{Si} directly diffuses through exchanging with its nearest neighbor, as shown in Fig. 1(b). Due to the lack of obstacles along the diffusion path, the diffusion process has a significant small diffusion barrier of ∼0.28 eV, suggesting a fast diffusion behavior of V_{Si} at room or working temperature.[40]

Different from the elemental semiconductor Si, the compound GaN consists of two sublattices. Structural anisotropy results in two different diffusion directions, i.e., diffusion along the c direction (polar axis, marked as path A) and diffusion within the ab plane (marked as path B). Here, all possible diffusion paths are considered as shown in Table I. For the case of V_{Ga}, the diffusion barrier along path A is 0.42 eV higher than that along with path B, and path B has the lowest diffusion barrier of ∼2.26 eV, as shown in

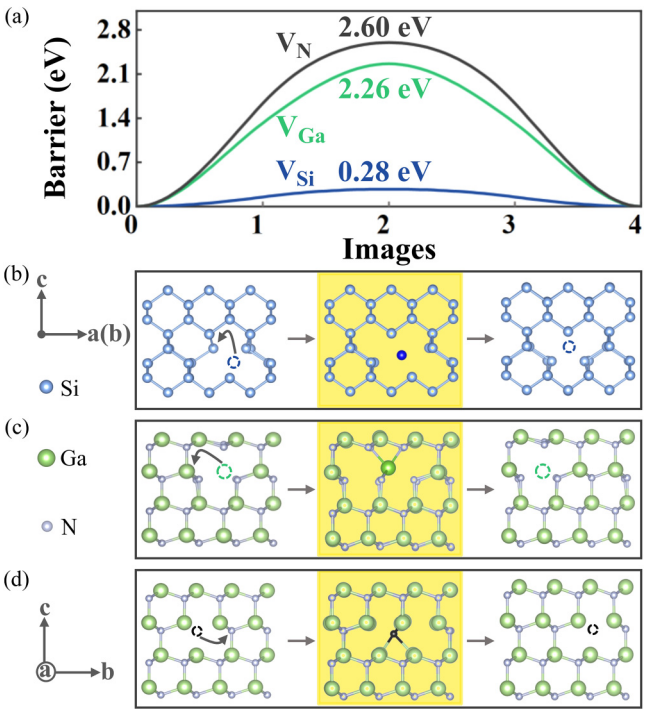

FIG. 1. Comparison of vacancy diffusions in Si and GaN. (a) The diffusion barriers of V_{Si} in Si and V_{Ga} and V_N in GaN. (b)–(d) The corresponding schematic diagram of the diffusion process along the lowest barrier path for V_{Si}, V_{Ga}, and V_N, respectively. Here, the left, yellow-shaded, and right regions correspond to the initial state, the saddle point, and the final state in the diffusion process, respectively. Dashed circles represent vacancies.

Figs. 1(a) and 1(c). Similar diffusion properties are also found for the case of V_N. Path B has the lowest diffusion barrier of ∼2.60 eV, slightly smaller than the diffusion barrier along with path A by 0.84 eV, as shown in Figs. 1(a) and 1(d). Compared to the diffusion of V_{Si} in Si, the diffusion of V_{Ga} and V_N along path B must cross the surrounding N and Ga atoms, as shown in Figs. 1(c) and 1(d), leading to significantly higher diffusion barriers. Meanwhile, the large diffusion barriers also imply that vacancies in GaN are unlikely to move at room or working temperature.

TABLE I. The diffusion barriers of defects along the c direction (path A) and the ab plane (path B) in GaN.

Defect	Path A (barrier/eV)	Path B (barrier/eV)
V_{Ga}	2.68	2.26
V_N	3.44	2.60
Ga_i	1.33	0.62
N_i	2.33	2.35

B. Diffusion mechanisms of individual interstitials in Si and GaN

Another kind of defect in semiconductors is the self-interstitial, which also contributes to the diffusion process,[21,22] suggesting its important role in the dynamic evolution of the defect. Considering the crystal symmetry of Si, there are three different interstitial positions, named as the hexagonal site (H-site), the split-interstitial site (S-site), and the tetrahedral site (T-site). The self-interstitials located in the T-site have much higher formation energy,[41] and the interstitials located in the H-site and S-site obey different diffusion mechanisms. As shown in Fig. 2(a), the H-site self-interstitial directly diffuses to the neighboring T-site and then to another equivalent H-site without the assistance of the host material, leading to a relatively small energy barrier of ∼0.31 eV. For the case of the S-site, however, the self-interstitial first kicks out the nearest-neighboring Si to form a new S-site and then moves through the interstitial channel, as shown in Fig. 2(b). Interestingly, the diffusion barrier of this kick-out diffusion mechanism is ∼0.33 eV, almost the same as the energy barrier of the straightforward diffusion of the H-site self-interstitials. Similar to the situation of individual vacancies, the small diffusion barriers imply that the diffusion of the self-interstitials in Si may occur easily and rapidly. For binary compound GaN, the most energy-favored Ga interstitial and N interstitial is the near octahedral site (O-site) and the split-interstitial site (S-site), respectively. Similar to the situation in Si, Ga_i also has two diffusion mechanisms, but the direct diffusion mechanism with a smaller diffusion barrier is the main diffusion mechanism, the corresponding energy barrier is 0.62 eV, and the kick-out diffusion mechanism is 1.33 eV, as shown in Figs. 2(c) and 2(d). However, only the kick-out diffusion mechanism can exist for the diffusion of N_i, as shown in Fig. 2(e). The interstitial N bonds with the N in the host to form the N—N dimer, and kicking out a neighboring N needs to break the N—N chemical bond, leading to a much higher diffusion barrier of ∼2.33 eV. The high diffusion barrier of ∼2.35 eV is also found along path B. As one can see, N_i prefers to stay without diffusion, and only the self-interstitial Ga_i diffuses relatively easily in GaN, in agreement with the experimental observation.[42] The migration barriers of V_{Ga}, V_N, and N_i are consistent with previous results.[29,30] In addition, the diffusion barrier of neutral Ga_i, which was not mentioned in previous studies, is also given. This also shows that our calculation results are reliable.

In general, the interstitial atom with a larger atomic radius will cause larger lattice distortion, resulting in a relatively larger diffusion barrier. However, it is unexpected to see that the diffusion barrier of Ga_i is much lower than that of N_i despite the larger atomic radius of the Ga atom. To further reveal the reason, we have calculated the electron localization function (ELF) to analyze the physical binding in the initial state and the saddle point. As one can see, the ELF of Ga_i with the direct diffusion mechanism is almost unchanged when the Ga_i moves from the initial state [left panel in Fig. 3(a)] to the saddle point [right panel in Fig. 3(a)], which reflects the almost no energy cost during the diffusion process, leading to a smaller energy barrier. Different from the case of Ga_i, the bond strength of the N—N dimer in the case of N_i will be greatly reduced when the N_i reaches the saddle point, as the

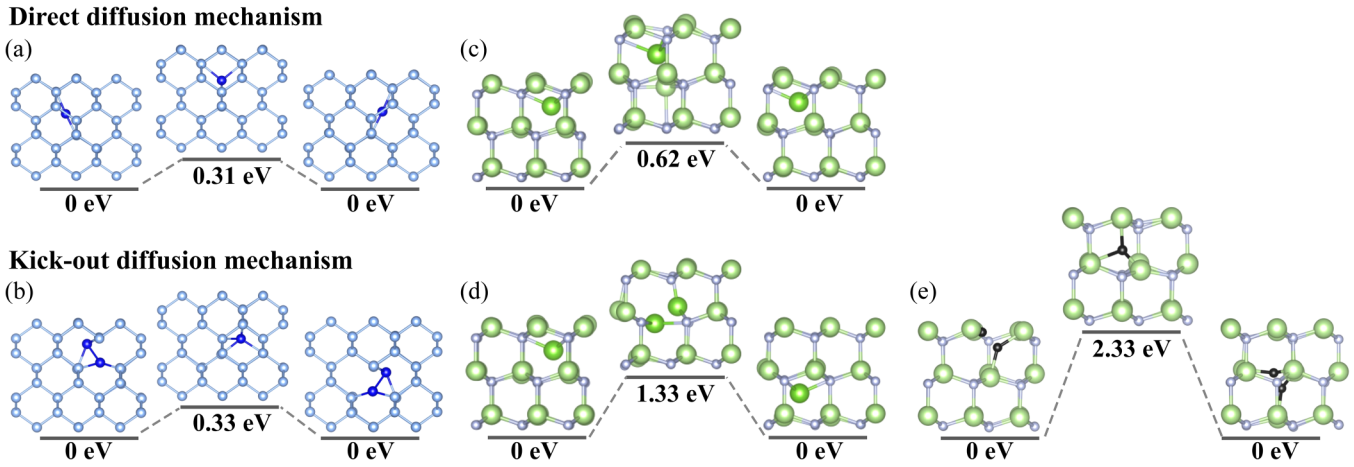

FIG. 2. Comparison of self-interstitials diffusion in Si and GaN. (a) and (c) The diffusion of Si_i and Ga_i via the direct diffusion mechanism, respectively. (b), (d), and (e) The diffusion of Si_i, Ga_i, and N_i via the kick-out diffusion mechanism, respectively.

results of the bond length of the N—N dimer change from 1.35 Å [between N≡N (1.10 Å) and N—N (1.47 Å)] at the initial state [left panel in Fig. 3(b)] to 1.95 Å at the saddle point [right panel in Fig. 3(b)]. The significant changes of bond energy for the case of N_i clearly illustrate that the strong N—N dimer bond needs to be broken during the migration process, which costs more energy and results in a larger energy barrier.

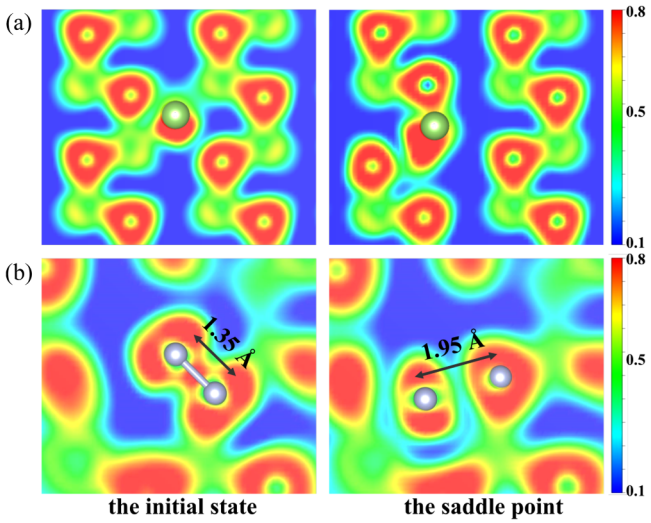

FIG. 3. Origins of the different diffusion barriers for Ga_i and N_i in GaN. (a) The calculated ELF for Ga_i in the initial state (left panel) and the saddle point (right panel). (b) The calculated ELF for N_i in the initial state (left panel) and the saddle point (right panel).

C. Recombination of vacancies and interstitials in Si and GaN

Both vacancies and self-interstitials can appear in one semiconductor, especially under complex nonequilibrium conditions like irradiations.[32] Therefore, it is necessary to develop a deep understanding of the recombination of vacancies and self-interstitials, which is crucial for the performance of semiconductor devices under extreme conditions. Here, we focus our discussion on the recombination between a single vacancy and interstitial defect pair to simplify our discussion.

In elemental semiconductor Si, V_{Si} and Si_i diffuse independently when they separate far away from each other. However, vacancies and interstitials can interact mutually when they are sufficiently close to each other, resulting in recombination of the V_{Si}–Si_i pair. Different from the tight-binding molecular dynamics,[43,44] we have performed the *ab initio* CI-NEB calculation to reveal the detailed process of recombination. As shown in Fig. 4(a), when Si_i diffuses close to V_{Si} (see inset A), V_{Si} migrates to the nearest-neighboring Si (marked by the purple ball) and Si_i also moves forward (see inset B), i.e., there is a synergistic effect to accelerate the recombination, as observed in previous studies,[43,44] but there is no V_{Si}–Si_i complex defect formation in our calculations. Finally, the recombination of the V_{Si}–Si_i pair happens (see inset C). It should be noted that the maximum energy barrier of the recombination is about ~0.32 eV. However, the recombination can result in a huge energy gain of ~7 eV. The small energy barrier and huge energy gain indicate that both V_{Si} and Si_i prefer to move and favor to recombine with each other in elemental semiconductor Si.

In the binary compound GaN, Ga_i with a smaller diffusion barrier can migrate to V_{Ga} or V_N through the direct diffusion mechanism. Considering the annealing temperature of GaN, the kick-out diffusion mechanism of Ga_i is also probable. Therefore, in the recombination process of the defect pair, we also involve the

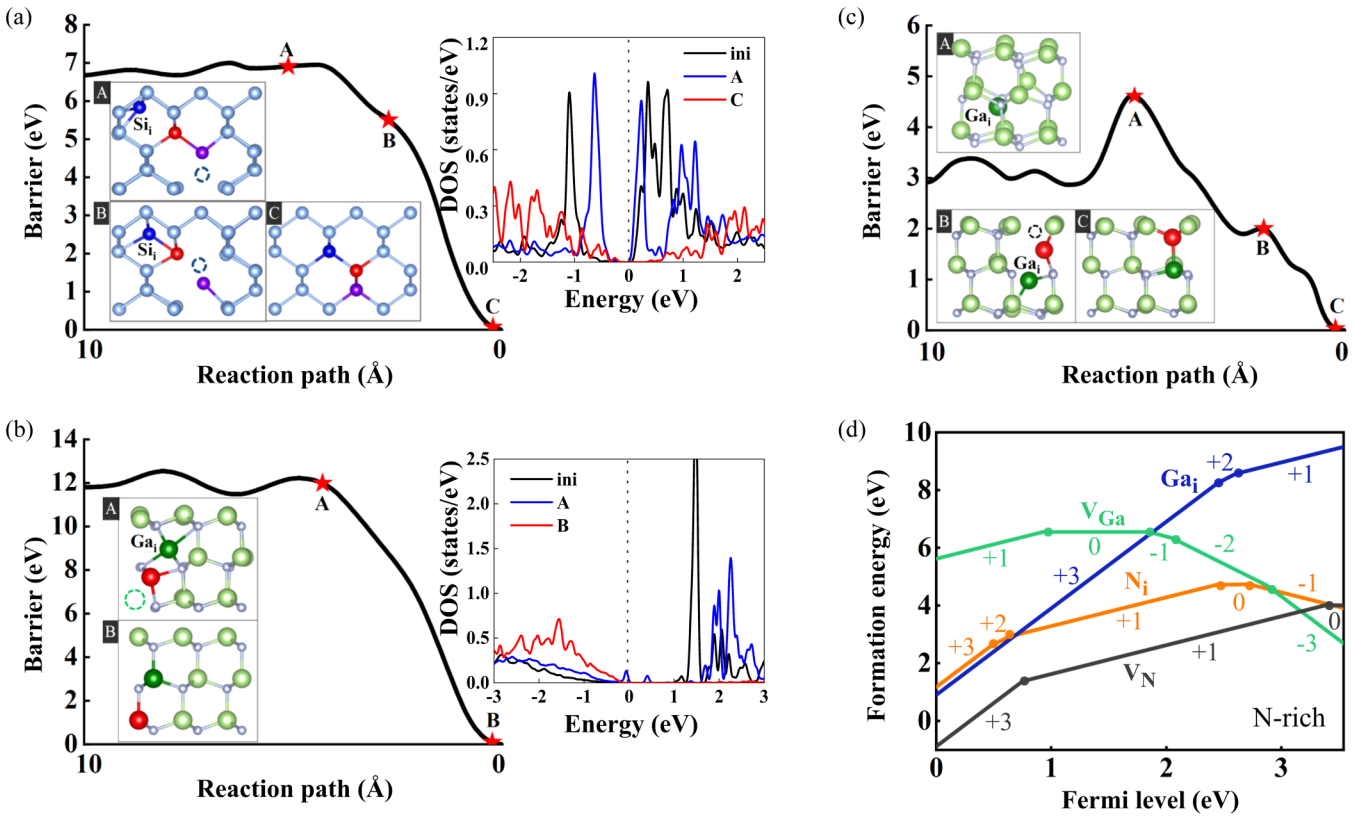

FIG. 4. Recombination of vacancies and interstitials in Si and GaN. The reaction paths of (a) V_{Si}–Si_i, (b) Ga_i–V_{Ga}, and (c) Ga_i–V_N as a function of the distance between defects. The insets are the snapshots at different recombination steps. The right panels of (a) and (b) show the DOS of Si_i in V_{Si}–Si_i and Ga_i in Ga_i–V_{Ga}, respectively, corresponding to the snapshot configurations (ini represents the initial state, that is, the interstitial and the vacancy are farthest apart). (d) Formation energies of V_{Ga}, V_N, N_i, and Ga_i as functions of the Fermi level.

kick-out diffusion mechanism. A similar recombination process is found for the Ga_i–V_{Ga} defect pair. As shown in Fig. 4(b), Ga_i moves close to V_{Ga} through the kick-out diffusion mechanism at first and then the recombination happens: Ga_i kicks out Ga in the host material (marked by the red ball) to form a new Ga_i (see inset A) and the new Ga_i recombines with V_{Ga} (see inset B). Different from recombination of the V_{Si}–Si_i pair in Si, which is caused by the synergistic effect of the diffusion of V_{Si} and Si_i, only the diffusion of Ga_i can contribute to the recombination of the Ga_i–V_{Ga} pair in GaN, as the significant energy barrier of V_{Ga} restricts its diffusion. As one can see, although the recombination of Ga_i–V_{Ga} can result in a huge energy gain of ∼12 eV, the energy barrier of 0.74 eV suggests that the recombination of Ga_i–V_{Ga} mainly occurs at the relatively high operating temperature.

Different from the V_{Si}–Si_i pair and the Ga_i–V_{Ga} pair, the recombination of the Ga_i–V_N pair in GaN is more complex. As shown in Fig. 4(c), Ga_i diffuses toward V_N through the kick-out diffusion mechanism and the direct approach simultaneously. When Ga_i reaches around V_N, the large lattice distortion caused by additional Ga due to its large atomic size will impede Ga_i from further getting close to V_N. The proximity effect causes a very large barrier of ∼1.75 eV, corresponding to the sharp peak at point A. After overcoming this energy barrier, the recombination is straightforward. Ga_i first kicks out one Ga in the host (see inset B). Then, the newly generated interstitial Ga recombines with V_N, generating a new defect Ga_N (see inset C). Although the recombination lowers the energy by ∼3 eV, it is unlikely to occur at the room or operating temperature of GaN due to the proximity effect with a large energy barrier.

Based on the above calculations, we can conclude that V_{Si} and Si_i both have a smaller diffusion barrier and V_{Si}–Si_i is easy to annihilate in Si. However, in GaN, only Ga_i can diffuse, and it can only recombine with V_{Ga} under the operating temperature. Therefore, after the annihilation process, the possible residual defects in GaN are N_i, V_{Ga}, and V_N. Then, we calculate the formation energies and CTLs of the residual defects and Ga_i in Fig. 4(d). Ga_i has two transition levels in the gap: $\varepsilon(3+/2+)$ and $\varepsilon(2+/1+)$. V_{Ga} has the lowest formation energy in n-type GaN and the deep level $\varepsilon(2-/3-)$ is 2.87 eV above the VBM. V_N has stable charge states 0, +1, and +3, and the transition level $\varepsilon(1+/3+)$ indicates a

TABLE II. Diffusion barriers for V_{Ga}^{2-}, V_N^{1+}, Ga_i^{2+}, and N_i along the c direction (path A) and the ab plane (path B) in GaN under $E_F = 2.53$ eV.

Defect	Path A (barrier/eV)	Path B (barrier/eV)
V_{Ga}^{2-}	2.36	1.95
V_N^{1+}	3.99	3.49
Ga_i^{2+}	1.11	0.94
N_i	2.33	2.35

"negative-U" character, agreeing with the previous conclusion.[45] Our calculations also show that N_i has four transition levels within the bandgap and has fairly high formation energies at different Fermi levels. When $E_F = 2.53$ eV, there are both charged V_{Ga}^{2-}, V_N^{1+}, and Ga_i^{2+} and neutral N_i defects in GaN; their diffusion barriers are shown in Table II, and the diffusion mechanism and diffusion paths are exactly the same as that of the neutral state. Furthermore, the density of states (DOS) of the interstitial atom in the defect pair, as shown in the right panel of Fig. 4(b). Compared with the defect state of Ga_i in the initial state , when Ga_i moves toward V_{Ga} (inset A), due to the interaction between V_{Ga} and Ga_i, the position of the defect state changes and the intensity of DOS decreases. When the defect pair recombines, the lattice recovers to the perfect lattice (inset B) and the defect state disappears completely. The DOS variation of Si_i is shown in the right panel of Fig. 4(a), which is similar to Ga_i. The changes in defect states during defects diffusion may reflect the evolution of the electronic structures of the materials.

Based on the above discussion, the dynamical evolutions of intrinsic defects in elemental Si and binary compound GaN can be illustrated clearly. The small diffusion barriers of V_{Si} and Si_i cause faster diffusion of these intrinsic defects in Si. Both V_{Si} and Si_i prefer to move and participate in the recombination, leading to the easier annihilation of the V_{Si}–Si_i defect pair, as shown in Fig. 5(a). Faster annihilation indicates that the elemental Si has an excellent self-recovery capability that might contribute to the relatively good performance of silicon devices under irradiation. Unlike elemental Si, most intrinsic defects are difficult to diffuse owing to the relatively high energy barriers, and only Ga_i prefers to move, leading to inefficient recombination even at a higher operating temperature, as shown in Fig. 5(b). On the other hand, the high energy barrier caused by the proximity effect further impedes the recombination of the Ga_i–V_N pair that will cause a new Ga_N defect, even at a high working temperature of GaN [see Fig. 5(b)]. Therefore, the recombination is ineffective in GaN, resulting in many residual defects like N_i, V_N, and V_{Ga}. Compared with elemental Si, it is expected that the self-recovery capability of the binary compound GaN is relatively weak; it might also partially account for the single event effect in GaN under irradiation.[46]

D. Comparison with the experimental observations under irradiations

For Si, the diffuse x-ray scattering investigation of irradiation-induced point defects in the experiment found that Si_i introduced by ion irradiation migrates at ~150 K with a ~0.3 eV migration activation energy, and V_{Si} moves at ~175 K with a similar magnitude migration energy.[31] These data are similar to our calculated ones. Importantly, the change of the diffuse scattering intensities under electron irradiation may indicate the recombination of Frenkel defects in Si,[31] and our calculations also support the efficient recombination of Frenkel defects in Si.

For GaN, first, annealing of negatively charged V_{Ga}, which is related to the isolated V_{Ga} becoming mobile with a migration barrier of ~1.8 eV.[47] This is in line with our calculation results (1.95 eV) and the migration barrier of V_{Ga} is much larger than that

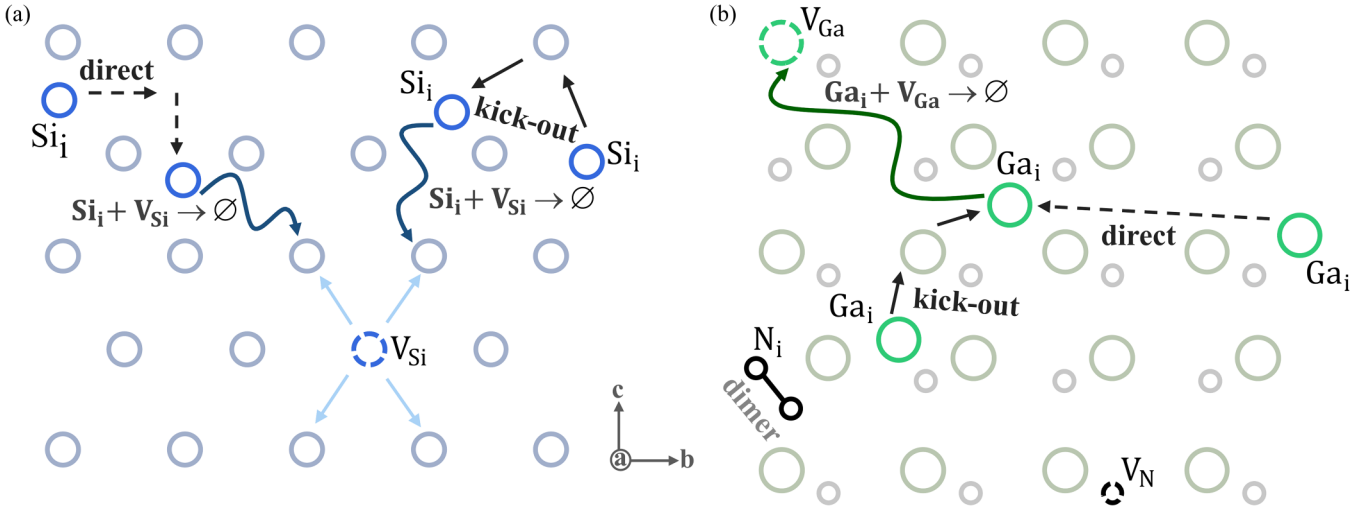

FIG. 5. Schematic diagram of the vacancies and interstitials recombination in (a) elemental Si and (b) binary compound GaN. The arrows indicate the migration of defects.

of V_{Si}. Second, the disordering rate of the Ga sublattice is smaller than the N sublattice,[34] which can also be understood in our theory that it mainly occurs on the Ga lattice, reducing its sublattice disorder. A significant recovery of the Ga disorder in the surface region is also observed under Si^{2+} ion irradiation, likely due to the assistance of the Frenkel pairs,[34] which according to our calculations are probably the recombination of Ga_i and V_{Ga}. These may suggest that the recovery capability of point defects in GaN is much lower than that of Si, as our calculation results.

IV. CONCLUSION

Based on the first-principles calculations, we have performed a comparative study on the diffusion mechanisms of point defects in Si and GaN. The different diffusion and recombination mechanisms of defects in Si and GaN are revealed. Importantly, a novel synergistic effect to accelerate the annihilation of defects is solely observed in Si, resulting in an efficient self-recovery mechanism in Si. Our results not only can provide important insight for the further understanding of the similarities and differences between these two material systems but also may explain some existing experimental observations for Si and GaN, especially under irradiation.

ACKNOWLEDGMENTS

We acknowledge the helpful discussion with Dr. J. F. Wang. This work was supported by the NSF of China (NSFC) (Grant Nos. 12088101 and 11634003) and NSAF (Grant No. U1930402). All the calculations were done in the Tianhe-JK cluster at CSRC.

AUTHOR DECLARATIONS

Conflict of Interest

The authors have no conflicts to disclose.

Author Contributions

Xiang-Ru Han: Investigation (lead); Writing – original draft (equal). **Yang Li:** Investigation (supporting). **Pei Li:** Investigation (supporting). **Xiao-Lan Yan:** Investigation (supporting). **Xiao-Qiang Wu:** Investigation (supporting). **Bing Huang:** Writing – original draft (equal).

DATA AVAILABILITY

The data that support the findings of this study are available from the corresponding author upon reasonable request.

REFERENCES

[1]P.-J. Ribeyron, Nat. Energy **2**, 17067 (2017).
[2]J. Bullock, Y. Wan, Z. Xu, S. Essig, M. Hettick, H. Wang, W. Ji, M. Boccard, A. Cuevas, C. Ballif, and A. Javey, ACS Energy Lett. **3**, 508 (2018).
[3]I. Massiot, A. Cattoni, and S. Collin, Nat. Energy **5**, 959 (2020).
[4]V. Adinolfi and E. H. Sargent, Nature **542**, 324 (2017).
[5]S. Pimputkar, J. S. Speck, S. P. DenBaars, and S. Nakamura, Nat. Photonics **3**, 180 (2009).
[6]G. Li, W. Wang, W. Yang, Y. Lin, H. Wang, Z. Lin, and S. Zhou, Rep. Prog. Phys. **79**, 056501 (2016).
[7]H. W. Hou, Z. Liu, J. H. Teng, T. Palacios, and S. J. Chua, Sci. Rep. **7**, 46664 (2017).
[8]C. Zhou, A. G. Melton, E. Burgett, N. Hertel, and I. T. Ferguson, Sci. Rep. **9**, 17551 (2019).
[9]G. D. Watkins and J. W. Corbett, Phys. Rev. **138**, A543 (1965).
[10]S. J. Pearton, R. Deist, F. Ren, L. Liu, A. Y. Polyakov, and J. Kim, J. Vac. Sci. Technol. A **31**, 050801 (2013).
[11]H. J. Queisser and E. E. Haller, Science **281**, 945 (1998).
[12]E. R. Weber, Physica B **340–342**, 1 (2003).
[13]J. S. Park, S. Kim, Z. Xie, and A. Walsh, Nat. Rev. Mater. **3**, 194 (2018).
[14]J. M. Ball and A. Petrozza, Nat. Energy **1**, 16149 (2016).
[15]S.-H. Wei, Comput. Mater. Sci. **30**, 337 (2004).
[16]C. Freysoldt, B. Grabowski, T. Hickel, J. Neugebauer, G. Kresse, A. Janotti, and C. G. V. de Walle, Rev. Mod. Phys. **86**, 253 (2014).
[17]P. Rinke, A. Janotti, M. Scheffler, and C. G. V. de Walle, Phys. Rev. Lett. **102**, 026402 (2009).
[18]L. Sun, M. R. G. Marques, M. A. L. Marques, and S. Botti, Phys. Rev. Mater. **5**, 064605 (2021).
[19]H. J. von Bardeleben, J. L. Cantin, U. Gerstmann, A. Scholle, S. Greulich-Weber, E. Rauls, M. Landmann, W. G. Schmidt, A. Gentils, J. Botsoa, and M. F. Barthe, Phys. Rev. Lett. **109**, 206402 (2012).
[20]C. G. V. de Walle and J. Neugebauer, J. Appl. Phys. **95**, 3851 (2004).
[21]A. Chroneos and H. Bracht, Appl. Phys. Rev. **1**, 011301 (2014).
[22]R. Ishikawa, R. Mishra, A. R. Lupini, S. D. Findlay, T. Taniguchi, S. T. Pantelides, and S. J. Pennycook, Phys. Rev. Lett. **113**, 155501 (2014).
[23]L. Hu, B. Huang, and F. Liu, Phys. Rev. Lett. **126**, 176101 (2021).
[24]J. Ma and S.-H. Wei, Phys. Rev. Lett. **110**, 235901 (2013).
[25]H.-X. Deng, J.-W. Luo, S.-S. Li, and S.-H. Wei, Phys. Rev. Lett. **117**, 165901 (2016).
[26]P. Śpiewak and K. J. Kurzydłowski, Phys. Rev. B **88**, 195204 (2013).
[27]F. El-Mellouhi, N. Mousseau, and P. Ordejón, Phys. Rev. B **70**, 205202 (2004).
[28]Y. Bar-Yam and J. D. Joannopoulos, Phys. Rev. B **30**, 2216 (1984).
[29]S. Limpijumnong and C. V. de Walle, Phys. Rev. B **69**, 035207 (2004).
[30]A. Kyrtsos, M. Matsubara, and E. Bellotti, Phys. Rev. B **93**, 245201 (2016).
[31]P. Partyka, Y. Zhong, K. Nordlund, R. S. Averback, I. M. Robinson, and P. Ehrhart, Phys. Rev. B **64**, 235207 (2001).
[32]A. Y. Polyakov, S. J. Pearton, P. Frenzer, F. Ren, L. Liu, and J. Kim, J. Mater. Chem. C **1**, 877 (2013).
[33]S. O. Kucheyev, J. S. Williams, C. Jagadish, J. Zou, G. Li, and A. I. Titov, Phys. Rev. B **64**, 035202 (2001).
[34]W. Jiang, W. J. Weber, C. Wang, L. M. Wang, and K. Sun, Defect Diffus. Forum **226–228**, 91 (2004).
[35]G. Kresse and J. Furthmüller, Phys. Rev. B **54**, 11169 (1996).
[36]P. E. Blöchl, Phys. Rev. B **50**, 17953 (1994).
[37]J. P. Perdew, K. Burke, and M. Ernzerhof, Phys. Rev. Lett. **77**, 3865 (1996).
[38]J. Heyd, G. E. Scuseria, and M. Ernzerhof, J. Chem. Phys. **118**, 8207 (2003).
[39]G. Henkelman, B. P. Uberuaga, and H. Jónsson, J. Chem. Phys. **113**, 9901 (2000).
[40]H. J. Scheel and T. Fukuda, *Crystal Growth Technology* (John Wiley & Sons, Ltd., 2003), p. 239.
[41]M. Kaltak, J. Klimeš, and G. Kresse, Phys. Rev. B **90**, 054115 (2014).
[42]K. H. Chow, G. D. Watkins, A. Usui, and M. Mizuta, Phys. Rev. Lett. **85**, 2761 (2000).
[43]M. Tang, L. Colombo, J. Zhu, and T. D. de la Rubia, Phys. Rev. B **55**, 14279 (1997).
[44]M. T. Zawadzki, W. Luo, and P. Clancy, Phys. Rev. B **63**, 205205 (2001).
[45]J. L. Lyons and C. G. V. de Walle, npj Comput. Mater. **3**, 12 (2017).
[46]S. Yue, Z. Zhang, Z. Chen, X. Zheng, L. Wang, Y. Huang, Y. Huang, C. Peng, and Z. Lei, IEEE Trans. Electron Devices **68**, 2667 (2021).
[47]F. Tuomisto, V. Ranki, D. C. Look, and G. C. Farlow, Phys. Rev. B **76**, 165207 (2007).